Korean J. of Chem. Eng., **14**(5), 347-353 (1997)

APPROACH FROM PHYSICOCHEMICAL ASPECTS IN MEMBRANE FILTRATION

Eiji Iritani[†] **and Yasuhito Mukai**

Department of Chemical Engineering, Nagoya University, Nagoya 464-01, Japan
(Received 19 May 1997 • accepted 20 June 1997)

Abstract – In membrane filtration, solution environment factors such as pH and solvent density are important in controlling the filtration rate and the rejection of the particles and/or the macromolecules. The filtration rate and the rejection in membrane filtration have been investigated from physicochemical aspects. It was shown that the properties of the filter cake formed on the membrane surface play a vital role in determining the filtration rate in membrane filtration. It was clearly demonstrated that such filtration behaviors as the filtration rate and the rejection are highly dependent on the electrical nature of the particles and/or the macromolecules. Furthermore, it was shown that the solvent density ρ has a large effect on the steady filtration rate in upward ultrafiltration.

Key words: Membrane Filtration, Filter Cake, pH, Ultrafiltration, Solvent Density

INTRODUCTION

The membrane filtration of colloidal solutions has become increasingly important in widely diversified fields. The appropriate control of both the filtration rate and the rejection (or the transmission) of the particles and/or the macromolecules in the membrane filtration process is of great interest in both industry and academia. While there exist many factors influencing the filtration behaviors [Fane, 1986], the underlying phenomena are currently not well understood.

The filtration behaviors are strongly affected by the properties of the filter cake formed by the accumulation of solutes on the membrane surface [Iritani et al., 1991a]. Therefore, an understanding of the cake structure can serve as a basis for clarifying the real mechanism of membrane filtration. Our results indicated that the cake structure is greatly influenced by the physicochemical properties, for instance, the nature of the interactions between solutes [Iritani et al., 1991a]. Especially when more than one type of solute is present in the solution, the situation becomes quite complex. For example, in the separation process, when larger solutes are present, solutes whose molecular dimensions are small enough to permeate the membrane are substantially retained [Iritani et al., 1995a].

The subject of this study is to relate the filtration behaviors to the structural properties of the filter cake obtained by using a batchwise filter which has a sudden reduction in its filtration area. The flux decline and the characteristic values of the cake in unstirred dead-end ultrafiltration are evaluated by use of analytical ultracentrifuge on the basis of the compressible cake resistance model. Also, the influence of pH on the flux decline in particulate microfiltration and protein ultrafiltration is studied. Next, we attempt to clarify the role of the solution environment in fractionation of binary protein mixtures by ultrafiltration. Lastly, the role of the solvent density in dead-end upward ultrafiltration is discussed by studying the dependence of the sedimentation behavior in ultracentrifugation experiments on the solvent density.

[†]To whom all correspondence should be addressed.

CAKE PROPERTIES IN MICROFILTRATION OF RUTILE SUSPENSIONS

In particulate microfiltration, as the model particle, we used titanium dioxide (Wako Pure Chemical Ind. Corp.) of the rutile form with the original mean specific surface area size of 0.47 μm. Fig. 1 shows the pH dependence of the zeta potential of rutile particles measured using a particle microelectrophoresis apparatus (Model 5-17, Mitamura Riken Ind. Corp.). It is clear from the figure that the isoelectric point of rutile particle, where the particle carries no charge, is at ca. 8.1.

The microfiltration experiments were conducted under con-

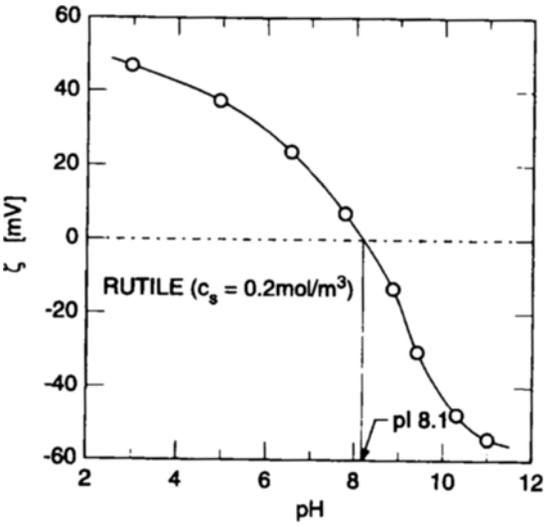

Fig. 1. Zeta potential ζ for rutile as function of pH.

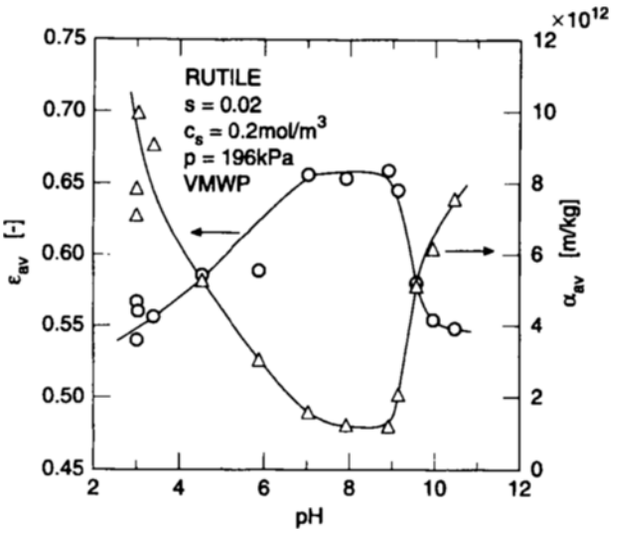

Fig. 2. Effect of pH on average porosity ε_{av} and average specific filtration resistance α_{av} of filter cake formed in microfiltration of rutile suspensions.

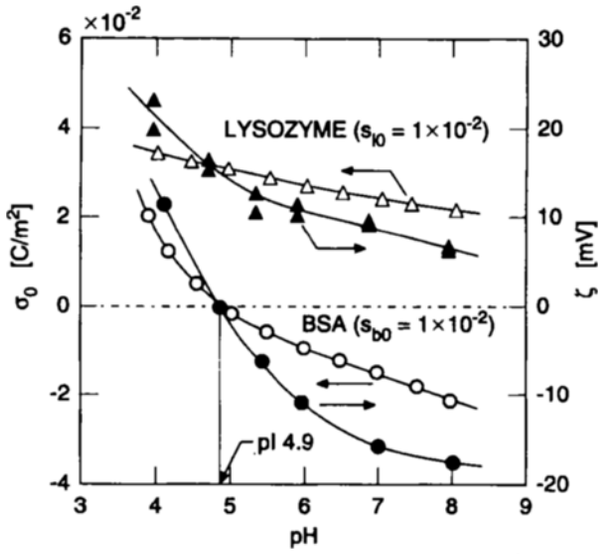

Fig. 3. Surface charge density σ_0 and zeta potential ζ for BSA and lysozyme as function of pH.

dition of constant pressure of 196 kPa, and the variations of the filtrate volume over time were measured with an electronic balance. As soon as the whole slurry was filtered, both the mass W_w of the wet cake and the mass W_d of the dry cake were measured. Thus, the average porosity ε_{av} of the cake was obtained by

$$\varepsilon_{av} = \frac{\rho_s(W_w - W_d)}{\rho_s(W_w - W_d) + \rho W_d} \quad (1)$$

where ρ_s is the true density of the solid, and ρ is the density of the filtrate. Microfiltration membranes (VMWP) with a nominal pore size of 0.05 μm, supplied by Millipore Corp., were used.

In Fig. 2, both the average porosity ε_{av} and the average specific filtration resistance α_{av} of the filter cake are plotted against pH. It can be seen that ε_{av} goes through a maximum around the isoelectric point. It is important to note that a loose filter cake provides a small hydraulic flow resistance. Thus, α_{av} is much smaller near the isoelectric pH.

Since the rutile particles are hydrophobic colloids, they are destabilized around the isoelectric point, and the very porous flocs are then formed. The filter cake formed from such porous flocs has often loose and wet structures [Iritani et al., 1997]. Consequently, the filter cake formed around the isoelectric point is more porous than that formed by the charged particles outside the isoelectric point.

CAKE PROPERTIES IN ULTRAFILTRATION OF BSA SOLUTIONS

In protein ultrafiltration, as one model protein, we used bovine serum albumin (BSA) (fraction V, Katayama Chemical Ind. Corp.) with a molecular weight of ca. 67,000 Da and with an isoelectric point of 4.9. In order to measure the average porosity of the filter cake accurately, the experiments were conducted using an unstirred batch filtration cell in which the filtration area was suddenly reduced at the distance of 0.4 mm from the membrane surface [Iritani et al., 1991a]. The experiments were conducted under constant pressure conditions, and the variations of the filtrate volume over time were measured with an electronic balance. In the apparatus, when the cake surface reaches the position where the filtration area is reduced, the filtration rate decreases suddenly. Therefore, the average porosity of the cake can be obtained by using the material balance of filtration. Asymmetric polysulfone membranes (PTTK) with a nominal molecular weight cut-off of 30,000 Da supplied by Millipore Corp. were employed.

Fig. 3 shows the pH dependence of the surface charge density σ_0 and the zeta potential ζ of the proteins. The zeta potential of the protein was measured using the electrophoretic light scattering method developed by Otsuka Electronics Corp. Also, the surface charge density on the protein was obtained by proton titration measurements conducted by addition of 0.1 N hydrochloric acid or sodium hydroxide. It is clear that the isoelectric point of BSA is about 4.9.

Fig. 4 shows the effect of pH on the properties of the filter cake formed in ultrafiltration of the BSA solution. It is of interest and significance that the results are in contrast to those for the rutile particles. It is clear that the lowest porosity occurs around the isoelectric point. Thus, α_{av} is much larger near the isoelectric point.

Since the BSA molecules are hydrophilic colloids, their stability in the solution would appear to be influenced not only by the presence of a surface charge on the protein but also by hydration of the surface layers of the protein. Thus, the BSA molecules have water bound to them even around the isoelectric point. The hydrophilic BSA molecules maintain a dispersed state in the solution due to hydration of the surface layers of the protein even around the isoelectric point. When a BSA molecule acquires a charge, the filter cake becomes loose and wet due to electrostatic repulsion between the charged BSA molecules. This contrasts to the compact cake around the isoelectric point.

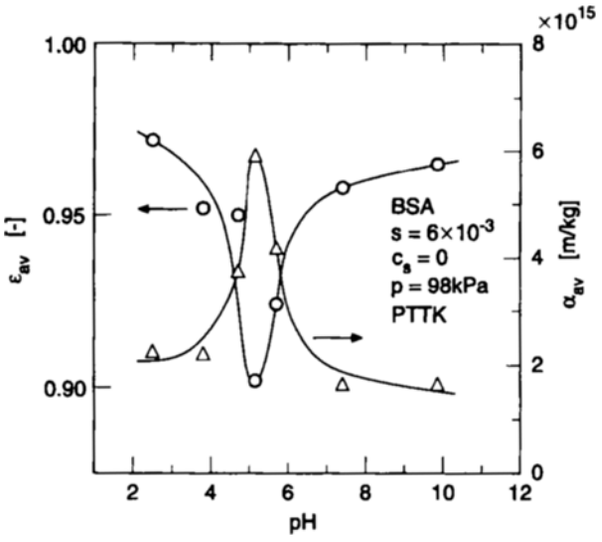

Fig. 4. Effect of pH on average porosity ε_{av} and average specific filtration resistance α_{av} of filter cake formed in ultrafiltration of BSA solutions.

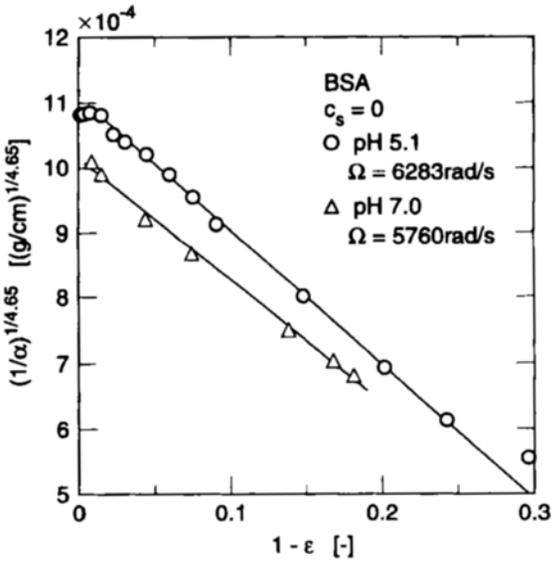

Fig. 5. Relation between local specific flow resistance α and porosity ε of solution.

ANALYSIS OF DEAD-END ULTRAFILTRATION BASED ON ULTRACENTRIFUGATION METHOD

In order to evaluate the flux decline and the cake structure in ultrafiltration of protein solutions, analytical ultracentrifugation experiments [Iritani et al., 1993, 1994, 1996] were conducted in a Hitachi Model 282 ultracentrifuge equipped with an optical system. The rotor speed ranged from 45,000 to 60,000 min ^{1}. The distributions of the concentration, the concentration gradient, and the refractive index gradient of the solutions in a 1.5 mm double-sector centerpiece were measured over time using both the ultraviolet scanner absorption system and Schlieren optics. In the sedimentation velocity experiment, the sedimentation velocity was determined from the displacement of the sedimentation boundary. In the high-speed sedimentation equilibrium experiment, the equilibrium thickness of the sediment of macromolecular solutes was measured after equilibrium was reached at a constant rotor speed.

At relatively high solution concentrations, there is an analogy between the sedimentation of a macromolecule in a solvent and the permeation of a solvent through the filter cake of macromolecules. The local specific flow resistance α can be calculated as [Iritani et al., 1993, 1994]

$$\alpha = \frac{(\rho_s - \rho)\, r_i \Omega^2}{\mu \rho_s v_0} = \frac{\rho_s - \rho}{\mu \rho_s S} \tag{2}$$

where r_i is the radial distance of the sedimentation boundary from the center of rotation, Ω is the angular velocity of the rotor, μ is the viscosity of the solvent, v_0 is the sedimentation velocity, and S is the sedimentation coefficient.

Thus, the relation between α and the volume fraction $(1-\varepsilon)$ of the solute may be written as [Iritani et al., 1993, 1994; Michaels and Bolger, 1962]

$$(1/\alpha)^{1/4.65} = \left(\frac{\rho_s d_f^2}{18 C_h}\right)^{1/4.65} \{1 - C_h(1-\varepsilon)\} \tag{3}$$

where d_f is the average equivalent spherical diameter of solutes, C_h is the ratio of the volume of the hydrous protein molecule to volume of anhydrous protein molecule, and ε is the porosity of the solution.

Fig. 5 shows the permeability data obtained by measuring the sedimentation velocities for a number of different solution concentrations. The plots are virtually linear as would be expected from Eq. (3). It is apparent that α around the isoelectric point is much smaller than that at pH 7 with the same solution concentration. On the other hand, as shown previously, the average specific filtration resistance α_{av} of the cake in the ultrafiltration of BSA solutions reaches a definite maximum around the isoelectric point. In order to account for this discrepancy, we conducted a high-speed sedimentation equilibrium experiment.

If the local solute concentration of the cake formed in ultrafiltration is known, then the specific flow resistance α of the cake can be evaluated by using the permeability data. Therefore, it is necessary to evaluate the local solute concentration of the cake. We thus determined the compression data representing the relation between the local porosity ε and the local solute compressive pressure p_s from high-speed sedimentation equilibrium experiments. If ε is related to p_s by Eq. (4), the equilibrium thickness $(R - r_s)$ of the sediment is related to the centrifugal acceleration $R\Omega^2$ by Eq. (5) [Iritani et al., 1993, 1994; Murase et al., 1989].

$$1 - \varepsilon = E p_s^{\beta} \qquad p_s \geq p_{si} \tag{4}$$

$$R - r_s = \frac{\omega_0^{1-\beta}}{E(1-\beta)} \{(\rho_s - \rho) R\Omega^2\}^{-\beta} \tag{5}$$

where R is the distance from the center of rotation to the bottom of the sediment, r_s is the distance from the center of rotation to the surface of the sediment, and ω_0 is the net solute volume of the entire sediment per unit cross-sectional area. Below p_{si}, ε is assumed to be constant, and is equal to the porosity at pressure p_{si}.

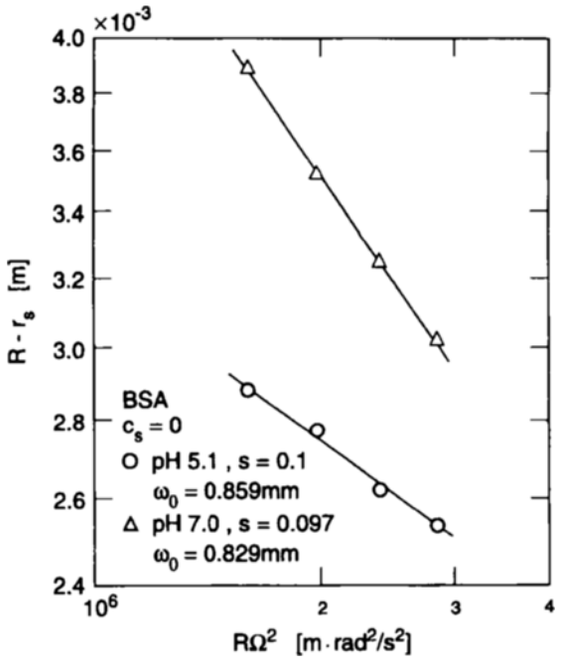

Fig. 6. Relation between equilibrium thickness ($R - r_s$) of sediment and centrifugal acceleration $R\Omega^2$.

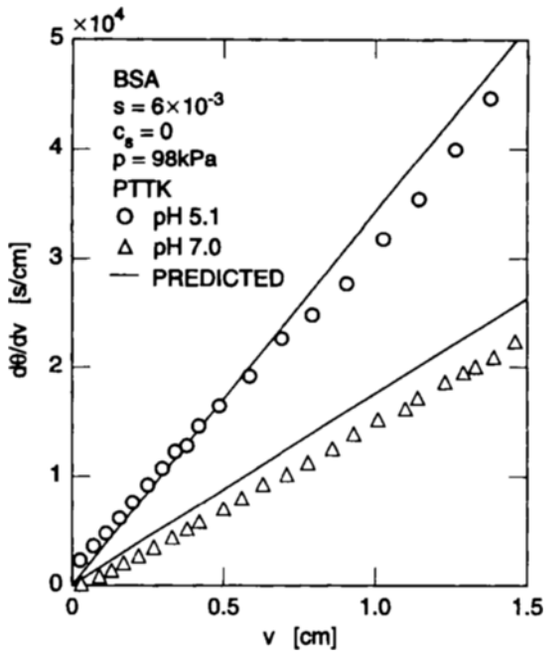

Fig. 7. Reciprocal filtration rate ($d\theta/dv$) as function of filtrate volume v per unit membrane area.

Fig. 6 represents the logarithmic plot of the equilibrium thickness ($R - r_s$) of the sediment against the centrifugal acceleration $R\Omega^2$. The plot shows a linear relationship in accordance with Eq. (5). It is interesting to note that the sediment at the isoelectric point is much more compact than that at pH 7 because the BSA molecule carries no net charge at the isoelectric point. Therefore, it would be expected that in protein ultrafiltration a compact filter cake forms around the isoelectric point. The relation between ε and p_s can be determined from the plot in the figure using Eqs. (4) and (5). On the basis of these relations, the variations of the filtration rate in ultrafiltration of protein solutions can be determined from the compressible cake resistance model [Iritani et al., 1991a, 1993; Shirato et al., 1969].

In Fig. 7, the results of unstirred dead-end ultrafiltration are plotted in the form of the reciprocal filtration rate ($d\theta/dv$) versus the filtrate volume v per unit membrane area. The filtration rate around the isoelectric point is much smaller than that at pH 7. The solid lines indicate the theoretical predictions based on the compression-permeability data obtained in analytical ultracentrifugation. The experimental data are in relatively good agreement with the theory, indicating that the compressible cake resistance model accurately describes the ultrafiltration behavior.

Fig. 8 shows the variations of the mass fraction c of the solute across the cake calculated on the basis of the ultracentrifugation data. In the compressible cake resistance model, the solutes deposited on the membrane are treated as the cake, and it is attributed to the hydraulic barrier. The cake tends to have a much more compact structure at the membrane in comparison to the relatively loose condition at the surface because the cake is compressible. Of considerable practical interest is that this result is in agreement with that obtained for cake filtration of particulate suspensions [Shirato et al., 1971]. A much more compact filter cake exhibiting a large resistance to flow may form around the isoelectric point than that which forms at pH 7. Consequently, the filtration rate at the isoelectric point becomes lower than that at pH 7.

CAKE PROPERTIES IN ULTRAFILTRATION OF BINARY PROTEIN MIXTURES

The properties of the cake formed on the retentive membranes in dead-end ultrafiltration of binary protein mixtures have been studied by using a mixture of the two proteins BSA and egg white lysozyme (Nagase Biochemical Ind. Corp.) [Iri-

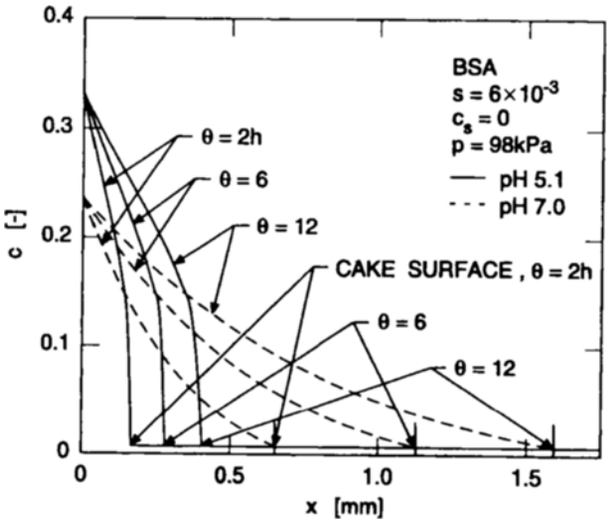

Fig. 8. Distributions of solute concentration c in filter cake.

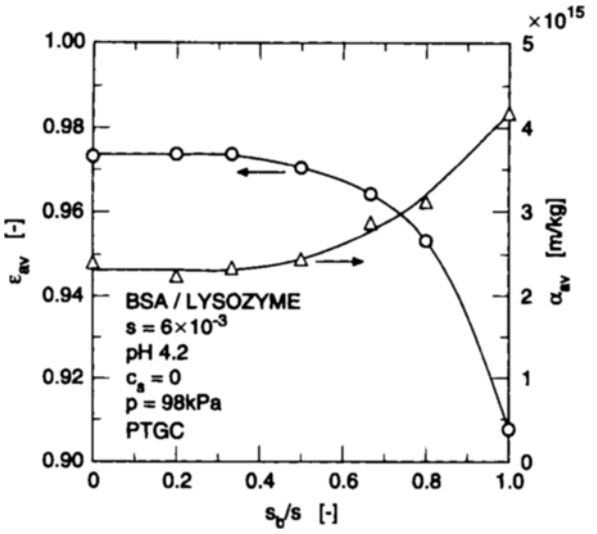

Fig. 9. Dependence of average porosity ε_{av} and average specific filtration resistance α_{av} on mixing ratio s_b/s of proteins in ultrafiltration of binary protein mixtures at pH 4.2.

tani et al., 1995b]. The molecular weight and the isoelectric point of lysozyme are 14,300 Da and 11.0, respectively. It can be seen from Fig. 3 that the lysozyme molecule has a net positive charge within the experimental range of the solution pH. Hydrophobic, polysulfone membranes (PTGC, Millipore Corp.) were employed. The membranes are claimed to display a nominal molecular weight cut-off of 10,000 Da, making it essentially impermeable to both solutes.

In Fig. 9, the properties of the filter cake at pH 4.2 are shown against the mixture ratio of the proteins, where s_b is the mass fraction of BSA in the solution, and s is the mass fraction of total solutes in solution. Both proteins are electropositive at that pH. It is clear that the average porosity ε_{av} is quite large. This is because only the electrostatic repulsive force acts between the macromolecules forming the cake at that pH. The decrease of the porosity ε_{av} roughly corresponds to the increase of the resistance α_{av}.

In Fig. 10, the typical results of ultrafiltration of the mixed protein solutions at pH 6.9 are illustrated. The results are in contrast to those shown in Fig. 9. Of particular importance is the surprising result that the porosity ε_{av} shows a distinct minimum. In the case of the single solute solutions, the average porosity is relatively large, since only an electrostatic repulsive force acts between the solutes. In contrast, in the mixed protein solutions, the BSA and lysozyme molecules are oppositely charged at pH 6.9. Therefore, the average porosity of the cake decreases markedly by adding the other protein to the single protein solution because of a higher attraction between solutes. The resistance shows a definite maximum at the mixing ratio of about 0.6 because the most compact cake forms at that mixing ratio. Therefore, the structure of the filter cake has a major impact on the ultrafiltration rate. To our knowledge, this is the first reported case which has clarified the relation between the cake structure and the filtration rate in ultrafiltration of binary protein mixtures.

FRACTIONATION PROPERTIES OF BSA AND LYSOZYME BY ULTRAFILTRATION

The conventional downward ultrafiltration, where the filtrate flow is in the same direction to gravity, and the newly developed upward ultrafiltration [Iritani et al., 1991b, 1992], where the filtrate flow is in the opposite direction to gravity, were conducted in an unstirred batch cell. Hydrophobic, polysulfone membranes (PTTK, Millipore Corp.) were employed. The membrane has a nominal molecular weight cut-off of 30,000 Da, making it essentially impermeable to BSA, but permeable to lysozyme. The variations of the filtrate weight

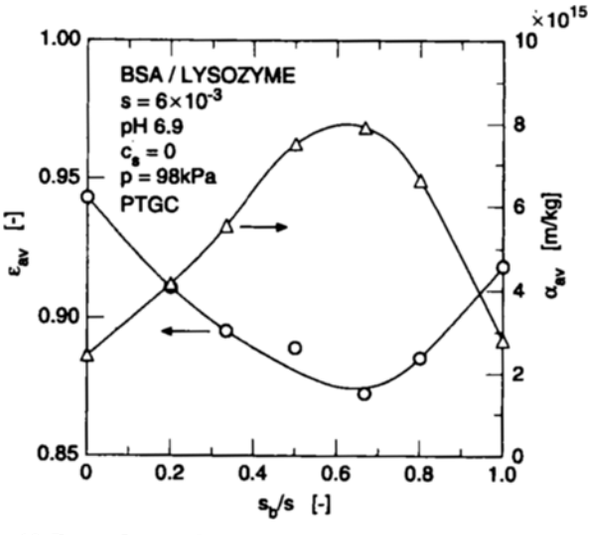

Fig. 10. Dependence of average porosity ε_{av} and average specific filtration resistance α_{av} on mixing ratio s_b/s of proteins in ultrafiltration of binary protein mixtures at pH 6.9.

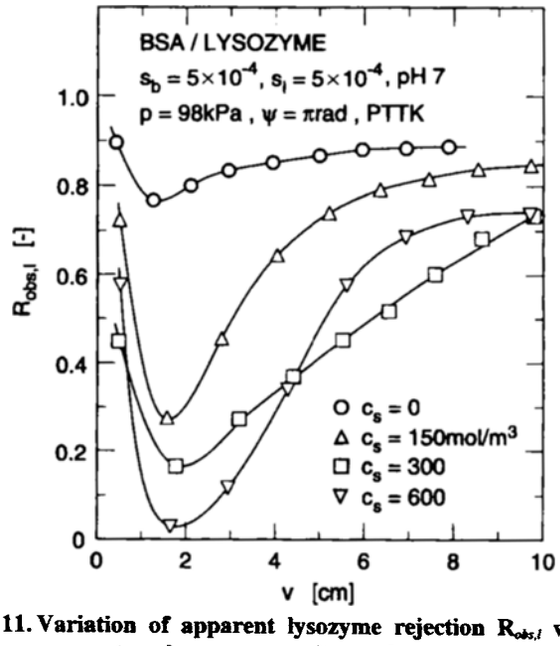

Fig. 11. Variation of apparent lysozyme rejection $R_{obs,l}$ with permeate volume v per unit membrane area at pH 7.

and each concentration of the two proteins in the filtrate were measured with time.

In Fig. 11, the apparent lysozyme rejection $R_{obs,l}$ in ultrafiltration of binary protein mixtures containing equal amounts of each protein is plotted against the cumulative filtrate volume v per unit membrane area, where c_s is the concentration of sodium chloride in the solution. The rejection is high during ultrafiltration in the absence of sodium chloride. The BSA molecule is negatively charged at pH 7, while the lysozyme molecule has a net positive charge. The filter cake consists of the mixture of the two proteins very well packed because of the attractive force associated with oppositely charged solutes. This results in the high rejection of lysozyme. The lysozyme rejection decreases by the addition of sodium chloride because charge-shielding between the protein molecules reduces the electrostatic attraction between BSA and lysozyme molecules. It should be emphasized that fractionation behaviors are largely affected by the solution environment [Iritani et al., 1995a].

ROLE OF SOLVENT DENSITY IN ULTRAFILTRATION BEHAVIOR

In upward ultrafiltration, the density of the protein molecules is an important factor influencing the filtration rate [Iritani et al., 1992, 1994]. In Fig. 12, the product of the steady filtration rate q_e in upward ultrafiltration and the viscosity μ is plotted against the density ρ of the solvent. The density of the solvent was adjusted by adding appropriate amounts of sucrose. The plots are remarkably linear. It is extremely important to note that increases in ρ bring about decreases in μq_e. Steady conditions in upward ultrafiltration may be achieved because the cake is exfoliated continuously. Such a phenomenon is caused by the gravitational force acting on the macrosolutes comprising the cake. Therefore, such an effect becomes more pronounced with smaller density of the solvent. It is of interest to note that extrapolation to $\mu q_e=0$ leads to the value of the buoyant density of the solute in its solution

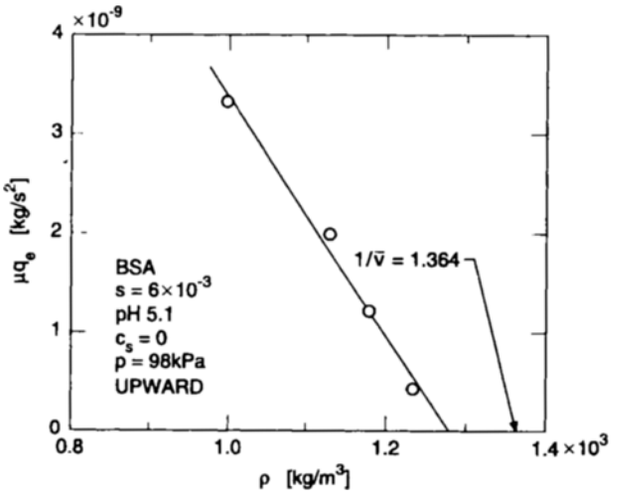

Fig. 12. Effect of density ρ of solvent on steady filtration rate q_e in upward ultrafiltration of protein solutions.

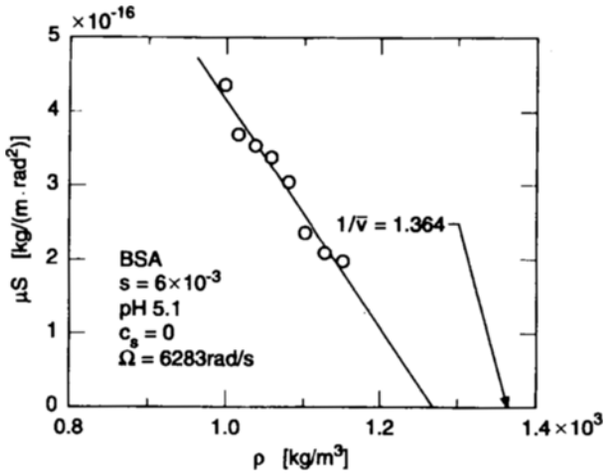

Fig. 13. Effect of density ρ of solvent on sedimentation coefficient S in ultracentrifugation of protein solutions.

environment. The dry density of BSA is 1.364 g/cm^3 [Peters, 1985]. The buoyant density obtained from the upward ultrafiltration experiments is smaller than the dry density due to hydration of the protein.

We can also obtain the buoyant density of the protein solute by ultracentrifugation experiments. In Fig. 13, the product of the sedimentation coefficient S in ultracentrifugation and the viscosity μ is plotted against the density ρ of the solvent. The plots are remarkably linear, as indicated by Eq. (2). Extrapolation to $\mu S=0$ leads to the value of the buoyant density of the solute. The most striking result is that this value is in excellent agreement with that obtained from the upward ultrafiltration experiments.

CONCLUSIONS

The properties of the cake formed on the retentive membranes were investigated for microfiltration of the particulate suspensions and ultrafiltration of protein solutions. The results demonstrated that the electrostatic interactions between solutes play a vital role in determining the filtration behaviors. On the basis of an analytical ultracentrifugation, the variations of the filtration rate and the properties of the filter cake in dead-end ultrafiltration were evaluated well using a compressible cake resistance model.

The characteristics of the ultrafiltration of the mixtures of BSA and lysozyme were investigated by using the retentive membrane and BSA-impermeable, lysozyme-permeable membrane. The results demonstrated that the electrostatic interactions between dissimilar molecules may control the filtration rate and the solute rejection significantly.

It was shown that the solvent density ρ has a significant effect on the steady filtration rate in upward ultrafiltration just as it does on the sedimentation coefficient in ultracentrifugation.

NOMENCLATURE

C_h : ratio of volume of hydrous protein molecule to volume

of anhydrous protein molecule
c : mass fraction of solute in filter cake
c_s : concentration of sodium chloride [mol/m^3]
d_f : average equivalent spherical diameter of solute [m]
E : constant in Eq. (4) [Pa$^{-\beta}$]
p : applied filtration pressure [Pa]
p_{si} : pressure below which ε remains constant [Pa]
p_s : local compressive pressure acting on solute [Pa]
q_e : steady filtration rate [m/s]
R : distance from center of rotation to bottom of sedimentation [m]
R_{obs} : apparent rejection
r_i : radial distance of sedimentation boundary from center of rotation [m]
r_s : distance from center of rotation to surface of sediment [m]
S : sedimentation coefficient [s/rad^2]
s : mass fraction of solid or solute in slurry or solution
v : filtrate volume per unit effective membrane area [m]
v_0 : sedimentation velocity [m/s]
$\bar{v}$: partial specific volume [m^3/kg]
W_d : mass of dry cake [kg]
W_w : mass of wet cake [kg]
x : distance from membrane surface [m]

Greek Letters

α : local specific filtration resistance [m/kg]
α_{av} : average specific filtration resistance [m/kg]
β : constant in Eq. (4)
ζ : zeta potential [V]
ε : local porosity
ε_{av} : average porosity
θ : filtration time [s]
μ : viscosity of solvent [Pa·s]
ρ : density of filtrate [kg/m^3]
ρ_s : density of solid or solute [kg/m^3]
σ_0 : surface charge density [C/m^2]
φ : angle between filtrate flow and direction of gravity [rad]
Ω : angular velocity [rad/s]
ω_0 : net solute volume of entire filter cake per unit effective membrane area [m]

Subscripts

b : BSA
l : lysozyme

REFERENCES

Fane, A. G., "Ultrafiltration: Factors Influencing Flux and Rejection", Progress in Filtration and Separation, Wakeman, R. J., ed., Elsevier, Amsterdam, **4**, 134 (1986).

Iritani, E., Hattori, K., Akatsuka, S. and Murase, T., "Sedimentation Behavior of Protein Solutions in Ultracentrifugation Field", *J. Chem. Eng. Japan*, **29**, 352 (1996).

Iritani, E., Hattori, K. and Murase, T., "Analysis of Dead-End Ultrafiltration Based on Ultracentrifugation Method", *J. Membrane Sci.*, **81**, 1 (1993).

Iritani, E., Hattori, K. and Murase, T., "Evaluation of Dead-End Ultrafiltration Properties by Ultracentrifugation Method", *J. Chem. Eng. Japan*, **27**, 357 (1994).

Iritani, E., Mukai, Y. and Murase, T., "Upward Dead-End Ultrafiltration of Binary Protein Mixtures", *Sep. Sci. Technol.*, **30**, 369 (1995a).

Iritani, E., Mukai, Y and Murase, T., "Properties of Filter Cake in Dead-End Ultrafiltration of Binary Protein Mixtures with Retentive Membranes", *Trans. IChemE*, **73**(A), 551 (1995b).

Iritani, E., Nakatsuka, S., Aoki, H. and Murase, T., "Effect of Solution Environment on Unstirred Dead-End Ultrafiltration Characteristics of Proteinaceous Solutions", *J. Chem. Eng. Japan*, **24**, 177 (1991a).

Iritani, E., Toyoda, Y. and Murase, T., "Effect of Solution Environment on Dead-End Microfiltration Characteristics of Rutile Suspensions", *J. Chem. Eng. Japan*, **30**, 614 (1997).

Iritani, E., Watanabe, T. and Murase, T., "Effects of pH and Solvent Density on Dead-End Upward Ultrafiltration", *J. Membrane Sci.*, **69**, 87 (1992).

Iritani, E., Watanabe, T. and Murase, T., "Upward and Inclined Ultrafiltration under Constant Pressure by Use of Dead-End Filter", *Kagaku Kogaku Ronbunshu*, **17**, 206 (1991b).

Michaels, A. S. and Bolger, J. C., "Settling Rates and Sediment Volumes of Flocculated Kaolin Suspensions", *Ind. Eng. Chem. Fundam.*, **1**, 24 (1962).

Murase, T., Iwata, M., Adachi, T., Gmachowski, L. and Shirato, M., "An Evaluation of Compression-Permeability Characteristic in the Intermediate Concentration Range by Use of Centrifugal and Constant-Rate Compression Techniques", *J. Chem. Eng. Japan*, **22**, 378 (1989).

Peters, T. Jr., "Serum Albumin", *Adv. Protein Chem.*, **37**, 161 (1985).

Shirato, M., Aragaki, T., Ichimura, K. and Ootsuji, N., "Porosity Variation in Filter Cake under Constant-Pressure Filtration", *J. Chem. Eng. Japan*, **4**, 172 (1971).

Shirato, M., Sambuichi, M., Kato, H. and Aragaki, T., "Internal Flow Mechanism in Filter Cakes", *AIChE J.*, **15**, 405 (1969).